Severe Molecular Defects of a Novel *FOXC1 W152G* Mutation Result in Aniridia

Yoko A. Ito,[1] *Tim K. Footz,*[1] *Fred B. Berry,*[1] *Farideh Mirzayans,*[1] *May Yu,*[1] *Arif O. Khan,*[2] *and Michael A. Walter*[1,3]

Purpose. *FOXC1* mutations result in Axenfeld-Rieger syndrome, a disorder characterized by a broad spectrum of malformations of the anterior segment of the eye and an elevated risk for glaucoma. A novel *FOXC1 W152G* mutation was identified in a patient with aniridia. Molecular analysis was conducted to determine the functional consequences of the *FOXC1 W152G* mutation.

Methods. Site-directed mutagenesis was used to introduce the *W152G* mutation into the *FOXC1* complementary DNA. The levels of W152G protein expression and the functional abilities of the mutant protein were determined.

Results. After screening for mutations in *PAX6, CYP1B1,* and *FOXC1*, a novel *FOXC1 W152G* mutation was identified in a newborn boy with aniridia and congenital glaucoma. Molecular analysis of the *W152G* mutation revealed that the mutant protein has severe molecular consequences in FOXC1, including defects in phosphorylation, protein folding, DNA-binding ability, inability to transactivate a reporter gene, and nuclear localization. Although *W152G* has molecular defects similar to those of the previously studied *FOXC1 L130F* mutation, *W152G* causes a more severe phenotype than *L130F*. Both the *W152G* and the *L130F* mutations result in the formation of protein aggregates in the cytoplasm. However, unlike the L130F aggregates, the W152G aggregates do not form microtubule-dependent inclusion bodies, known as aggresomes.

Conclusions. Severe molecular consequences, including the inability of the W152G protein aggregates to form protective aggresomes, may underlie the aniridia phenotype that results from the *FOXC1 W152G* mutation. (*Invest Ophthalmol Vis Sci.* 2009;50:3573–3579) DOI:10.1167/iovs.08-3032

The anterior segment of the eye consists of structures—iris, trabecular meshwork, Schlemm's canal—that are important for maintaining proper flow of aqueous humor. Many of these structures, including the iris stroma and the trabecular meshwork, are derived from the periocular mesenchyme. Differentiation of the periocular mesenchyme during development is under the influence of several transcription factors, including PAX6 and FOXC1.[1] Mutations in *PAX6* and *FOXC1* have been suggested to prevent the proper interaction of surface and neural ectodermal cells with neural crest-derived mesenchymal cells during development,[1] resulting in anterior segment dysgenesis. Specifically, mutations in *PAX6* have been implicated in aniridia (absence of the iris),[2] whereas mutations in *FOXC1* cause Axenfeld-Rieger Syndrome (ARS).[3] ARS includes a variety of ocular anomalies that affect the iris (hypoplasia, corectopia, polycoria, and peripheral anterior synechia) and other ocular structures. Patients with aniridia or ARS are at a high risk for glaucoma,[4,5] a progressively blinding condition that is usually associated with elevated intraocular pressure.

FOXC1 belongs to the *F*orkhead B*ox* family of transcription factors, which are characterized by a highly conserved DNA-binding Forkhead Domain (FHD). The FHD consists of three α-helices and two β-strands. Each β-strand is followed by a winglike loop. All missense mutations identified to date lie within the FHD. Molecular analyses of several of these *FOXC1* missense mutations suggest that the different subdomains within the FHD may have specific functional roles.[6]

A novel *FOXC1* missense mutation, W152G, was identified in a newborn boy with aniridia and congenital glaucoma. In this report, the W152G mutation was analyzed to understand how molecular defects in FOXC1 contribute to the development of ocular malformations, including aniridia. Furthermore, molecular analysis of the W152G mutation highlights the importance of having efficient quality control machinery within the cell that is able to regulate improperly folded protein.

Methods

Mutation Detection

The research adhered to the tenets of the Declaration of Helsinki. *PAX6* and *FOXC1* were amplified as previously described.[3,7] *CYP1B1* was amplified using previously published primers[8] and DNA polymerase (KAPAHiFi; Kapa Biosystems, Inc., Woburn, MA). Polymerase chain reaction (PCR) products were gel purified and extracted on separation columns (Qiagen, Valencia, CA). The coding regions of *PAX6, CYP1B1,* and *FOXC1* were sequenced using a genetic analyzer (3130*xl*; Applied Biosystems Inc., Foster City, CA) as previously described.[9]

Plasmid

Site-directed mutagenesis was performed (QuikChange mutagenesis kit; Stratagene, La Jolla, CA) with the addition of 10% dimethylsulfoxide. Mutagenic primer sequences for W152G were as follows: forward, 5′-ggcaagggcagctacgggacgctggacccgg-3′; reverse, 5′-ccgggtccagcgtcccgtagctgcccttgcc-3′. Potential mutant constructs were sequenced. Confirmed mutants were subcloned into the *FOXC1* pcDNA4 His/Max vector (Invitrogen, Burlington, ON, Canada),[10] and the entire insert was resequenced.

Cell Culture

COS-7 cells, HeLa cells, and nonpigmented ciliary epithelial cells were cultured in high-glucose Dulbecco's modified Eagle's medium (DMEM) and supplemented with 10% fetal bovine serum (FBS). Immortalized

From the Departments of [1]Medical Genetics and [3]Ophthalmology, University of Alberta, Edmonton, AB, Canada; and the [2]Pediatric Ophthalmology Division, King Khaled Eye Specialist Hospital, Riyadh, Saudi Arabia.

Supported by the Canadian Institutes of Health Research.

Submitted for publication October 17, 2008; revised February 2, 2009; accepted May 15, 2009.

Disclosure: **Y.A. Ito**, None; **T.K. Footz**, None; **F.B. Berry**, None; **F. Mirzayans**, None; **M. Yu**, None; **A.O. Khan**, None; **M.A. Walter**, None

The publication costs of this article were defrayed in part by page charge payment. This article must therefore be marked "*advertisement*" in accordance with 18 U.S.C. §1734 solely to indicate this fact.

Corresponding author: Michael A. Walter, 839 Medical Sciences Building, University of Alberta, Edmonton, AB, Canada, T6G 2H7; mwalter@ualberta.ca.

human trabecular meshwork (HTM) cells were cultured in low-glucose DMEM and 10% FBS.

Immunoblot Analysis

COS-7 or HeLa cells were transfected with 4 μg epitope-tagged (Xpress; Invitrogen) *FOXC1*[10] with the use of a reagent (Fugene 6; Roche, Mississauga, ON, Canada). Whole-cell extracts were prepared 48 hours after transfection, as described previously.[11] The proteins were resolved on an SDS-PAGE gel, transferred to a nitrocellulose membrane, and probed with the appropriate antibodies as described previously.[11] Epitope-tagged (Xpress; Invitrogen) FOXC1 was detected with anti–epitope-tagged (Xpress; Invitrogen) antibody (1:10,000). For the phosphorylation experiments, protein extracts were incubated with 20 U calf intestinal alkaline phosphatase (CIP; Invitrogen), with or without 11 μM sodium vanadate ($NaVO_3$), for 1 hour at 37°C before being resolved on an SDS-PAGE gel. Protein extracts were partially digested by incubation with 1.7 μM trypsin at 37°C for 5 minutes. Digestion products were resolved on an SDS-PAGE gel and were detected using a rabbit polyclonal antibody raised against FOXC1 (1:2000; Abcam, Cambridge, MA).

Immunofluorescence

Cells were grown and transfected directly on coverslips with 1 μg epitope-tagged (Xpress; Invitrogen) *FOXC1* as previously described.[10] Either 24 hours or 48 hours after transfection, the cells were fixed with 2% paraformaldehyde for 15 minutes and were processed for immunofluorescence as previously described.[12] The formation of protein aggregates was further analyzed by treatment of HTM cells with 20 μM MG132 and/or 0.01 μg/μL nocodazole 14 hours before processing for immunofluorescence. The FOXC1 protein was visualized by incubation with anti–epitope-tagged (Xpress; Invitrogen) antibody and anti–mouse Cy3-conjugated secondary antibody (Jackson ImmunoResearch, West Grove, PA) while the nucleus was visualized by incubation with DAPI. At least 100 cells were scored for each experimental group.

Electrophoretic Mobility Shift Assay (EMSA)

The amount of W152G protein in COS-7 whole cell extracts was equalized to wild-type (WT) FOXC1 levels by inspection of the proteins detected by immunoblotting. EMSA was performed as described previously.[10]

Transactivation Assay

The FOXC1 luciferase reporter assay was performed as described previously.[12] Each experiment was conducted three times in triplicate. Proper expression of all expression vectors was first verified by parallel immunoblot analysis.

Modeling

In silico mutagenesis of the FOXC2 FHD model (98% identical with the FOXC1 FHD) was performed with Swiss-Pdb Viewer (http://ca.expasy.org/spdbv/) and was evaluated with the Atomic Non-Local Environment Assessment (ANOLEA) server (http://www.swissmodel.expasy.org/anolea/)[13] as described previously.[9]

Results

A newborn boy had severe ocular malformations including bilateral megalocornea and opacity, aniridia, and congenital glaucoma (Figs. 1A–C).[14] The patient had no recorded family history of ocular disease. Given that aniridia has been associated with mutations in *PAX6*, we screened *PAX6* by direct sequence analysis of PCR products from the patient DNA. However, no *PAX6* mutations were found. Screening of *CYP1B1*, a gene that has been implicated in primary congenital glaucoma,[15] identified the following polymorphisms: rs2617266TT, rs10012GG, rs1056827TT, rs1056836CC, rs1056837CC, and rs1800440AG. All six alterations in *CYP1B1* have been reported to be non–disease-causing SNPs and thus, were unlikely to have contributed to the negative phenotypes in this patient. Subsequently, we screened *FOXC1* for mutations. A heterozygous T-to-G transversion at codon position 152 (c.454T>G; W152G) was identified (Fig. 1D). This mutation was confirmed by sequencing both strands of the amplified product. The W152G mutation was not present in 100 normal control chromosomes. This is the first reported case of a mutation involving an amino acid residue within β-strand 2 of the FOXC1 FHD and extends the phenotypic consequence of *FOXC1* mutations to include aniridia.

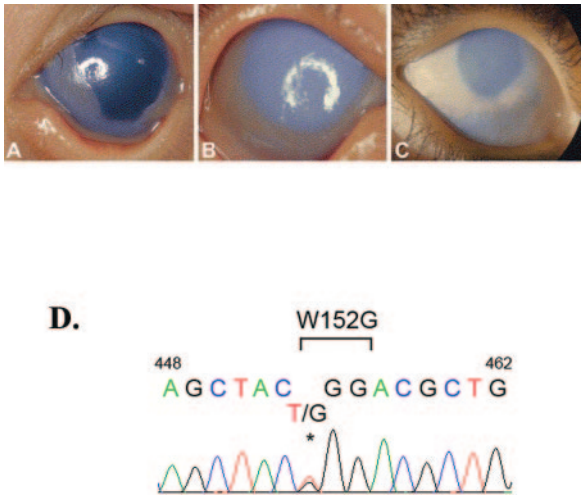

Figure 1. *FOXC1 W152G* mutation identified in a patient with aniridia. (**A**) At 2 weeks of age, abnormal elevated thickened limbal tissue and diffused corneal haze (stromal scarring, stromal edema, and epithelial edema) are observed. (**B**) At 2 months of age, the abnormal tissue is no longer distinct, there is no elevation of limbal tissue, and pannus is present ×360°. (**C**) At 5 months of age, the pannus is replaced by scarring. The photographs are reprinted from Al-Shahwan S, Edward DP, Khan AO. Severe ocular surface disease and glaucoma in a newborn with aniridia. *J AAPOS*. 2005;9:499–500. © 2005, with permission from the American Association for Pediatric Ophthalmology and Strabismus. (**D**) The chromotagram shows the genomic DNA sequence of the patient in (**A**–**C**). The patient has a heterozygous T-to-G transversion that results in a tryptophan-to-glycine change at codon position 152.

To examine how the W152G mutation alters FOXC1 function, the W152G mutation was introduced into the *FOXC1* cDNA by site-directed mutagenesis. The W152G protein is stable enough to be detected by immunoblot analysis (Fig. 2A). As we have previously reported, the WT FOXC1 protein migrates as multiple bands because of phosphorylated forms of the protein.[16] The W152G protein also occurred as multiple bands. However, one of the mutant bands had faster mobility than the WT bands. The WT and W152G FOXC1 proteins were incubated with calf intestinal alkaline phosphatase (CIP) to confirm that the multiple bands were attributed to phosphorylated forms of the FOXC1 protein. When the WT and W152G protein lysates were incubated with CIP, the presence of the upper band was reduced (Fig. 2B). Based on these data, we conclude that the W152G mutant protein may be folded or phosphorylated differently from the WT protein. Because neither tryptophan nor glycine can be phosphorylated, any difference in phosphorylation was not attributed to direct phosphorylation changes of this residue at position 152. Rather, changes that affected the entire protein structure, such as misfolding of the protein, could have been responsible. To examine this possibility, the WT and W152G FOXC1 proteins were partially digested with trypsin. Incubation of the protein lysates with

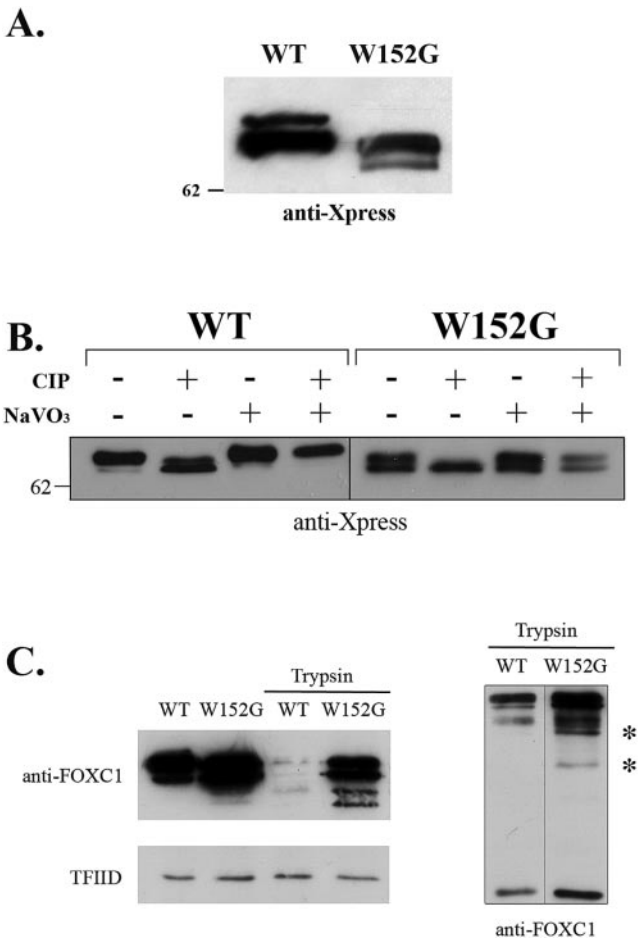

FIGURE 2. Expression analysis of WT and W152G FOXC1 cDNAs in transfected COS cells. (**A**) WT FOXC1 and W152G recombinant proteins were detected by immunoblotting. WT and W152G occurred as multiple bands, but the migration pattern of W152G was altered. (**B**) Treatment with CIP and $NaVO_3$ indicates that the upper band is attributed to phosphorylated forms of the protein for WT and W152G. (**C**, *left*) The immunoblot has equal protein loading. W152G is more resistant than WT when partially digested with trypsin. *Right*: to visualize the digestion products for WT and W152G, the immunoblot was loaded with equal protein expression levels. *Asterisks*: different digestion products between the WT and W152G proteins.

trypsin resulted in the disappearance of nearly all the full-length WT bands, whereas the full-length W152G bands were still visible (Fig. 2C, left), indicating that W152G results in a mutant FOXC1 protein with decreased accessibility to trypsin. This fact plus the observation of different digestion products of WT compared with W152G FOXC1 proteins suggest that there are differences in the overall structure of the WT and mutant proteins (Fig. 2C, right).

The DNA-binding ability of the W152G protein was examined by EMSA. The ability to bind to DNA is essential for FOXC1 to function as an effective transcription factor and to regulate the expression of other genes. As expected, the WT protein was able to bind to the FOXC1 binding site (Fig. 3A). However, the W152G protein was unable to bind even when the protein level was increased (Fig. 3A). Based on the EMSA results, we conclude that the W152G mutation greatly disrupts the DNA-binding ability of the mutant FOXC1 protein.

A reporter assay was conducted in HeLa cells to examine the ability of the W152G protein to activate a luciferase reporter gene containing six copies of the consensus FOXC1 binding sites. The transactivation ability of W152G was only 3% of WT FOXC1, similar to that of the empty expression vector (Fig. 3B).

The ability of the W152G FOXC1 protein to localize to the nucleus was examined by immunofluorescence. More than 90% of HTM cells showed exclusive nuclear localization of the FOXC1 WT protein (Fig. 4A). However, there was a dramatic reduction in the number of HTM cells with exclusive nuclear localization of the W152G FOXC1 protein (10.3%) compared with the WT protein (92%; Fig. 4A). Most cells showed localization of the W152G protein to both the nucleus and the cytoplasm. Interestingly, the W152G mutant proteins formed aggregated complexes in the cytoplasm in approximately 30% of cells (Fig. 4A). Aggregated complexes in the cytoplasm have been observed for one other FOXC1 mutation, L130F.[9] To examine whether the protein aggregates are part of aggresomes, we treated the cells with MG132, a proteasomal inhibitor known to induce the formation of aggresomes.[17] Because microtubules are essential for the formation of aggresomes, the cells were also treated with nocodazole, which disrupts microtubules.[17] The MG132 and nocodazole treatments did not affect the nuclear localization of the WT protein (Table 1; Fig.

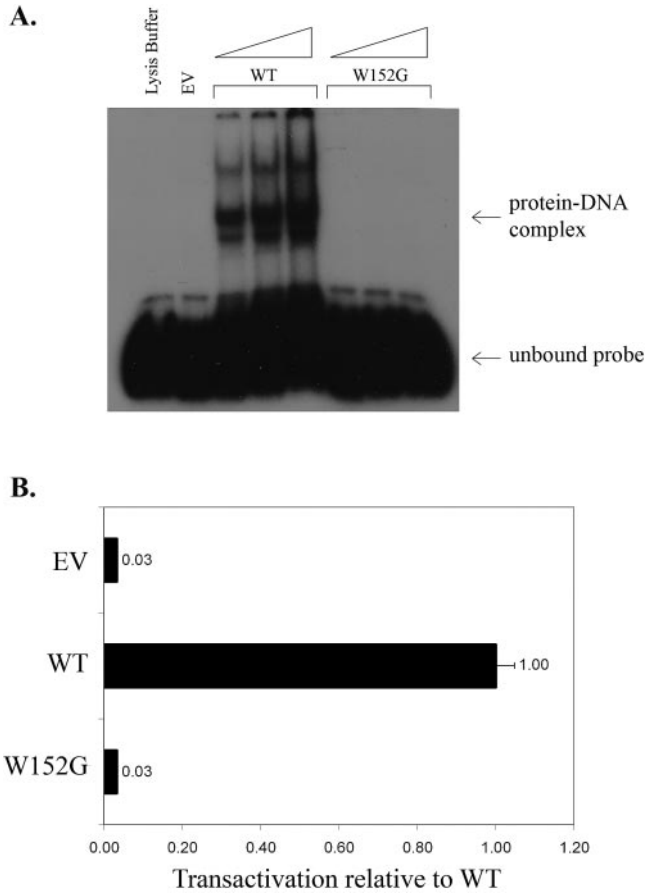

FIGURE 3. Molecular defects of the FOXC1 W152G mutant protein. (**A**) Whole-cell extracts from COS cells transfected with FOXC1 WT or FOXC1 W152G expression vectors were incubated with a radioactively labeled FOXC1 consensus binding site oligonucleotide probe. FOXC1 WT formed protein-DNA complexes, but FOXC1 W152G did not form protein-DNA complexes even when the amount of the FOXC1 W152G protein was increased. (**B**) The FOXC1 W152G mutant protein was unable to transactivate a firefly luciferase reporter gene with six copies of the in vitro-derived FOXC1-binding site. Firefly luciferase values were normalized to a *Renilla* luciferase control. Mean luciferase values from a representative experiment transfected in triplicate are shown. Error bars represent the SEM.

A.

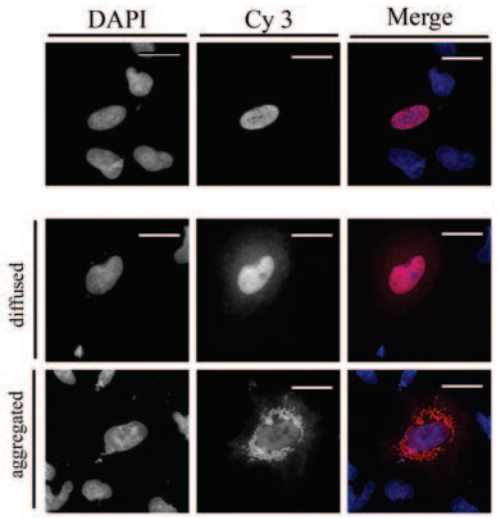

	Exclusive Localization (%)		Nucleus+Cytoplasm (%)	
	Nucleus	Cytoplasm	Diffuse	Aggregated
WT	92.0	0	8.0	0
W152G	10.3	0.4	60.1	29.2

B.

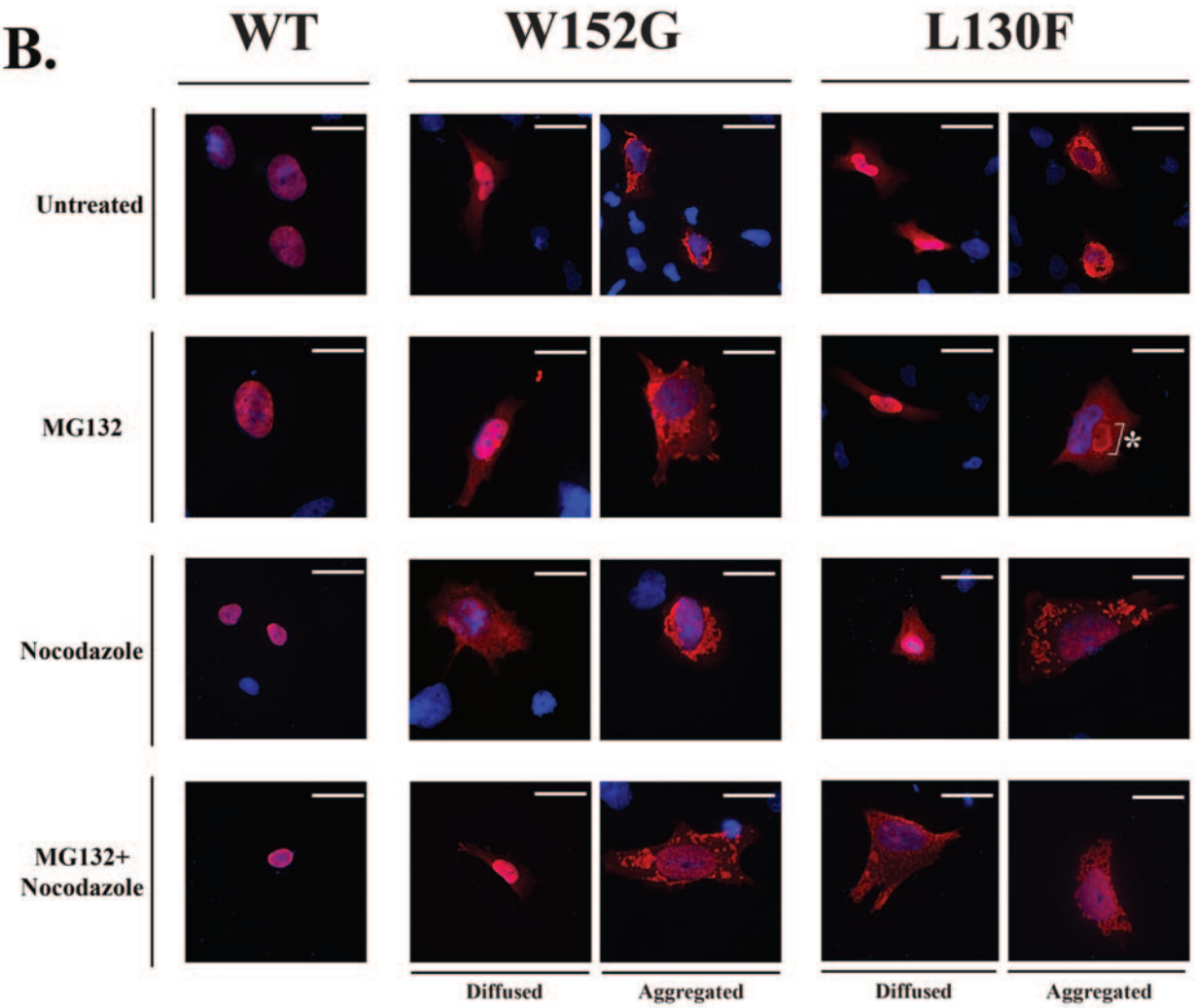

TABLE 1. Summary of Subcellular Localization of the WT, L130F, and W152G FOXC1 Proteins in HTM Cells Treated with or without MG132 and Nocodazole 48 Hours after Transfection

	No. of Cells Counted	Exclusive Localization (%)		Nucleus + Cytoplasm (%)	
		Nucleus	Cytoplasm	Diffused	Aggregated
WT untreated	107	84.1	0	15.9	0
WT+MG132	120	83.3	0	16.7	0
WT+NOC	132	84.8	0	15.2	0
WT+MG132+NOC	120	82.5	0	17.5	0
L130F untreated	104	15.4	0	38.5	46.2
L130F+MG132	104	12.5	0	37.5	50.0
L130F+NOC	102	3.9	0	62.7	33.3
L130F+MG132+NOC	106	13.2	0	50.9	35.8
W152G untreated	113	5.3	0	66.4	28.3
W152G+MG132	107	0	0.9	72.0	27.1
W152G+NOC	111	1.8	0	64.0	34.2
W152G+MG132+NOC	109	8.3	0	56.9	34.9

4B). MG132 treatment did not affect the formation of protein aggregates for either the W152G or the L130F mutation (Table 1). Interestingly, fully formed aggresomes were observed in MG132-treated HTM cells expressing L130F (Fig. 4B). Nocodazole treatment with or without MG132 decreased the percentage of cells with protein aggregates from 46.2% in untreated cells to 35.8% and 33.3%, respectively, for the L130F mutation. These results further verify that the L130F proteins form aggresomes. For the W152G mutation, adding nocodazole with or without MG132 did not decrease the number of cells with protein aggregates, suggesting that the protein aggregates formed by the W152G protein are not microtubule-dependent inclusion bodies (Table 1; Fig. 4B). Although both W152G and L130F result in the formation of protein aggregates in the cytoplasm, aggresome formation was only observed for the L130F mutation. These results suggest that the two mutant FOXC1 proteins are processed in the cell by different mechanisms.

FOXC2-based homology models[9] of the FOXC1 FHD bearing the L130F and W152G mutations were analyzed to determine potential effects on protein structure. Figure 5B shows a comparison of ANOLEA mean force potentials calculated for the mutations compared with WT. The analysis indicated that the L130F mutation was predicted to have unfavorable effects (i.e., higher ANOLEA scores) on the residues at positions 87, 130, and 152. However, W152G affects a different set of residues, namely those at positions 98, 99, 130, 136, 138, and 152. Therefore, it appears that W152G may cause a more profound disturbance to the structure of an important hydrophobic pocket of the FHD than L130F. This difference in the predicted effects on FOXC1 structure is consistent with the more severe molecular and phenotypic consequences of the W152G mutation.

DISCUSSION

In this study, we identified a novel *FOXC1* missense mutation, W152G, in a patient with aniridia and congenital glaucoma (Fig. 1A). This finding of a *FOXC1* mutation causing aniridia is supported by a recent report of another patient with aniridia with a FOXC1 M161K mutation.[18] However, FOXC1 M161K mutations were previously identified in two other patients, both of whom had ARS (iris hypoplasia, a prominent Schwalbe line, peripheral anterior synechiae) rather than aniridia,[19,20] indicating phenotypic variability in patients with FOXC1 M161K mutations. Distinguishing between the distinct phenotypes that can apparently rise from the same FOXC1 M161K mutation would be of interest for future studies.

This study on the FOXC1 W152G mutation is the first examination of the molecular consequences of an aniridia-causing *FOXC1* mutation. In addition, this is the first time a mutation has been found in a residue within β-strand 2 of the FOXC1 FHD. Interestingly, molecular modeling by Saleem et al.[10] predicted that the W152 residue forms highly conserved pairwise interactions with other hydrophobic amino acid residues, such as I87 and L130. These hydrophobic residues are involved in the formation of a hydrophobic core within the FHD. In addition to the novel W152G mutation, two mutations involving amino acid residues that form this hydrophobic core have been reported. Both I87M and L130F result in severe disruptions to normal FOXC1 protein function, including defects in protein stability, nuclear localization, and DNA binding.[9,10] Thus, amino acid residues involved in the formation of the hydrophobic core appear to be particularly important for the FOXC1 protein function.

Mutations often lead to the synthesis of misfolded proteins. Tryptophan and glycine are hydrophobic and neutrally charged amino acid residues. Despite these similarities, the W152G mutation appears to distort the protein structure by preventing the linear amino acid chain from folding properly. Molecular modeling predicts that substituting tryptophan with the much smaller glycine residue at codon position 152 results in a protein in a less energetically favorable state (Fig. 5). Such an energetically unfavorable state would be predicted to result in a misfolded protein.

FIGURE 4. Localization patterns of FOXC1 W152G and FOXC1 L130F proteins in HTM cells. (**A**) Most FOXC1 WT-expressing cells displayed a nuclear-exclusive pattern (*top*). However, 60.1% of FOXC1 W152G-expressing cells displayed a diffused pattern of mutant protein in the cytoplasm (*middle*), and 29.2% of cells displayed an aggregated pattern of proteins in the cytoplasm (*bottom*). (**B**) Neither MG132 nor nocodazole treatment affected the ability of the FOXC1 WT protein to localize exclusively to the nucleus. Neither MG132 nor nocodazole treatment of HTM cells transfected with FOXC1 W152G changed the characteristics of the protein aggregates. *Asterisk*: MG132 treatment induced the formation of aggresomes in HTM cells transfected with FOXC1 L130F (MG132, aggregated). Interestingly, although protein aggregates were still present in the cytoplasm of HTM cells treated with nocodazole (with or without MG132), the protein aggregates appeared to be more dispersed (compare nocodazole aggregated panel and MG132+nocodazole aggregated panel with untreated aggregated panel). *Blue*: DAPI-stained nuclei. *Red*: Cy3 fluorescence of epitope-tagged recombinant FOXC1 proteins. Scale bars, 10 μm.

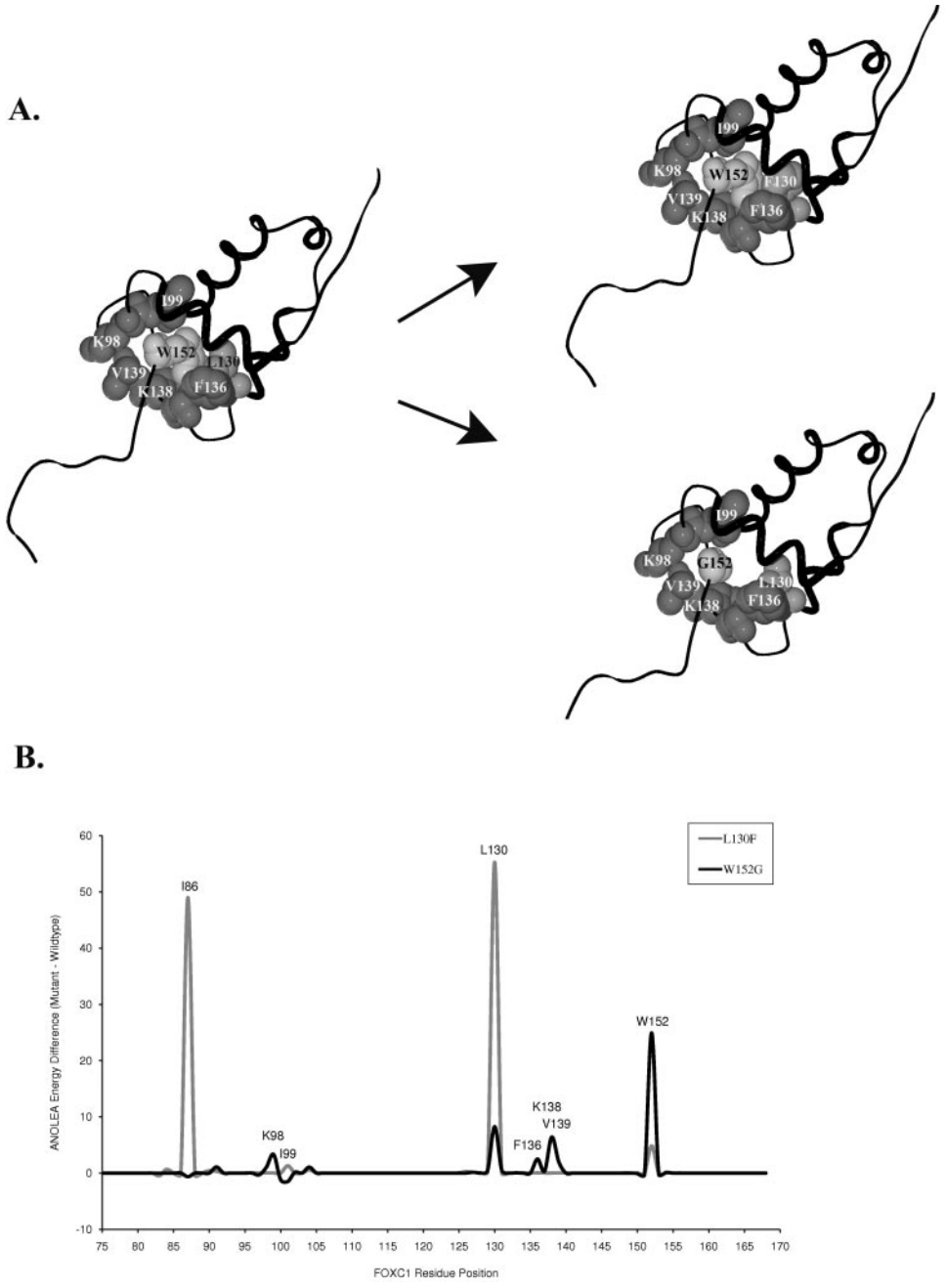

FIGURE 5. (**A**) Comparison of W152G and L130F molecular models. In silico mutagenesis shows that replacement of the bulky W152 side chain with glycine may result in suboptimal packing in the FHD hydrophobic core. The protein backbone is depicted in *black*, unmutated residues in *dark gray*, and position 152 in *light gray*. WT and mutant models were submitted to the ANOLEA Swiss model server. (**B**) Peaks on the scatter plot represent amino acid positions that experience an altered pseudoenergy state, as calculated by ANOLEA, as a result of the indicated mutation.

Supporting this prediction is the partial digest with trypsin that resulted in different digestion products between the WT and W152G proteins, thus indicating the proteins are folded differently (Fig. 2C). The W152G mutation could result in the exposure of normally hidden trypsin sites or, alternatively, could result in normally exposed trypsin sites becoming inaccessible. This may explain how trypsin cleaves the mutant protein at different sites compared with the WT protein, resulting in different digestion products (Fig. 2C). Thus, consistent with the molecular modeling prediction, the W152G mutation appears to alter the overall topology of the FOXC1 protein.

Misfolding of the mutant FOXC1 protein has severe consequences on normal FOXC1 protein function. Immunofluorescence results showed that most of the W152G proteins were unable to localize exclusively to the nucleus (Fig. 4A). These results were surprising because the W152G mutation is not located within the known nuclear localization signal (NLS) or nuclear localization accessory signal (NLAS).[16] FOXC1 mutations involving substitution of amino acid residues with the same charge usually result in milder nuclear localization defects than mutations that introduce an amino acid residue with a different charge.[6] The altered topology of the W152G protein could prevent the correct detection of the NLS and NLAS, preventing the protein from localizing to the nucleus. Interestingly, nocodazole treatment with or without MG132 decreased the number of cells with L130F protein aggregates (Table 1; Fig. 4B). Nevertheless, disassembling these protein aggregates did not result in increased exclusive nuclear localization of the L130F protein. Thus, at least in the case of the L130F mutation, the protein aggregates do not appear to contribute to the severity of the nuclear localization defect.

Many of the molecular defects caused by the *W152G* mutation are similar to the molecular defects observed with

the *L130F* mutation. The W152G and the L130F mutant proteins are phosphorylated differently than the WT protein, have a nuclear localization defect, and cannot bind to DNA.[9] In both cases, the net result is that the ability of FOXC1 to regulate gene expression is impaired. Despite these similarities, however, the *W152G* mutation and the *L130F* mutation cause different phenotypes. The *W152G* mutation causes aniridia and congenital glaucoma.[14] The *L130F* mutation was found in a woman with a mild form of ARS and no glaucoma.[9] Her son was diagnosed with a severe form of ARS (corectopia, hypertelorism, posterior embryotoxon) and congenital glaucoma.[9] A possible explanation for the difference in phenotype is that the L130F mutant proteins form aggresomes but the W152G proteins do not. In normal cells, the protein quality control machinery prevents the accumulation of protein aggregates by promoting correct folding of proteins through chaperone activity and continuously degrading misfolded proteins before protein aggregates can form.[21] Misfolding of the protein often results in the incorrect exposure of hydrophobic surfaces that are usually buried in the protein core.[22] When the misfolded form of the protein persists, such as when a mutation causes the misfolding, protein aggregates may form primarily through the incorrect intermolecular interaction of the hydrophobic surfaces of the misfolded proteins.[23] Because such protein aggregates are stable complexes that can be pathogenic,[21] some cells form aggresomes to protect against potentially toxic protein aggregates.[17] Aggresomes are cytoplasmic inclusion bodies that form when protein aggregates are transported by microtubules to the microtubule organizing center.[17] They may form when the capacity of the proteasomal degradation pathway is exceeded.[17] Kopito[21] suggests that concentrating the protein aggregates into aggresomes may promote the degradation of aggregates by autophagy, thereby providing an alternative route for the cell to discard potentially toxic protein aggregates. Thus, although the *L130F* mutation results in protein aggregates in approximately 18% more cells than the *W152G* mutation (Table 1; Fig. 4B), these cells may be able more effectively to discard the protein aggregates by forming aggresomes. As a result of an inability to participate in this additional degradation pathway, the *W152G* mutation may cause a more severe phenotype than the *L130F* mutation. The inability of the W152G protein aggregates to form aggresomes along with the numerous other molecular defects of the W152G protein may underlie the aniridia phenotype that results from the *FOXC1 W152G* mutation.

Acknowledgments

The authors thank Jonathan Chi for technical assistance and the members of the Walter Laboratory for critical input into the manuscript.

References

1. Cvekl A, Tamm ER. Anterior eye development and ocular mesenchyme: new insights from mouse models and human diseases. *Bioessays.* 2004;26:374–386.
2. Hanson IM, Fletcher JM, Jordan T, et al. Mutations at the PAX6 locus are found in heterogeneous anterior segment malformations including Peters' anomaly. *Nat Genet.* 1994;6:168–173.
3. Mears AJ, Jordan T, Mirzayans F, et al. Mutations of the forkhead/winged-helix gene, FKHL7, in patients with Axenfeld-Rieger anomaly. *Am J Hum Genet.* 1998;63:1316–1328.
4. Fitch N, Kaback M. The Axenfeld syndrome and the Rieger syndrome. *J Med Genet.* 1978;15:30–34.
5. Nelson LB, Spaeth GL, Nowinski TS, Margo CE, Jackson L. Aniridia: a review. *Surv Ophthalmol.* 1984;28:621–642.
6. Saleem RA, Banerjee-Basu S, Murphy TC, Baxevanis A, Walter MA. Essential structural and functional determinants within the forkhead domain of FOXC1. *Nucleic Acids Res.* 2004;32:4182–4193.
7. Mirzayans F, Pearce WG, MacDonald IM, Walter MA. Mutation of the *PAX6* gene in patients with autosomal dominant keratitis. *Am J Hum Genet.* 1995;57:539–548.
8. Acharya M, Mookherjee S, Bhattacharjee A, et al. Primary role of CYP1B1 in Indian juvenile-onset POAG patients. *Mol Vis.* 2006;12:399–404.
9. Ito YA, Footz TK, Murphy TC, Courtens W, Walter MA. Analyses of a novel L130F missense mutation in FOXC1. *Arch Ophthalmol.* 2007;125:128–135.
10. Saleem RA, Banerjee-Basu S, Berry FB, Baxevanis AD, Walter MA. Analyses of the effects that disease-causing missense mutations have on the structure and function of the winged-helix protein FOXC1. *Am J Hum Genet.* 2001;68:627–641.
11. Berry FB, Mirzayans F, Walter MA. Regulation of FOXC1 stability and transcriptional activity by an epidermal growth factor-activated mitogen-activated protein kinase signaling cascade. *J Biol Chem.* 2006;281:10098–10104.
12. Berry FB, O'Neill MA, Coca-Prados M, Walter MA. FOXC1 transcriptional regulatory activity is impaired by PBX1 in a filamin A-mediated manner. *Mol Cell Biol.* 2005;25:1415–1424.
13. Melo F, Feytmans E. Assessing protein structures with a non-local atomic interaction energy. *J Mol Biol.* 1998;277:1141–1152.
14. Al-Shahwan S, Edward DP, Khan AO. Severe ocular surface disease and glaucoma in a newborn with aniridia. *J AAPOS.* 2005;9:499–500.
15. Stoilov I, Akarsu AN, Sarfarazi M. Identification of three different truncating mutations in cytochrome P4501B1 (CYP1B1) as the principal cause of primary congenital glaucoma (buphthalmos) in families linked to the GLC3A locus on chromosome 2p21. *Hum Mol Genet.* 1997;6:641–647.
16. Berry FB, Saleem RA, Walter MA. FOXC1 transcriptional regulation is mediated by N- and C-terminal activation domains and contains a phosphorylated transcriptional inhibitory domain. *J Biol Chem.* 2002;277:10292–10297.
17. Johnston JA, Ward CL, Kopito RR. Aggresomes: a cellular response to misfolded proteins. *J Cell Biol.* 1998;143:1883–1898.
18. Khan AO, Aldahmesh MA, Al-Amri A. Heterozygous FOXC1 mutation (M161K) associated with congenital glaucoma and aniridia in an infant and a milder phenotype in her mother. *Ophthalmic Genet.* 2008;29:67–71.
19. Komatireddy S, Chakrabarti S, Mandal AK, et al. Mutation spectrum of FOXC1 and clinical genetic heterogeneity of Axenfeld-Rieger anomaly in India. *Mol Vis.* 2003;9:43–48.
20. Panicker SG, Sampath S, Mandal AK, Reddy AB, Ahmed N, Hasnain SE. Novel mutation in FOXC1 wing region causing Axenfeld-Rieger anomaly. *Invest Ophthalmol Vis Sci.* 2002;43:3613–3616.
21. Kopito RR. Aggresomes, inclusion bodies and protein aggregation. *Trends Cell Biol.* 2000;10:524–530.
22. Wetzel R. Mutations and off-pathway aggregation of proteins. *Trends Biotechnol.* 1994;12:193–198.
23. Markossian KA, Kurganov BI. Protein folding, misfolding, and aggregation: formation of inclusion bodies and aggresomes. *Biochemistry (Mosc).* 2004;69:971–984.